Haploinsufficiency of the Nijmegen breakage syndrome 1 gene increases mammary tumor latency and metastasis

ROWENA WAN and DAVID L. CROWE

University of Illinois Cancer Center, Chicago, IL 60612, USA

Received March 8, 2012; Accepted April 9, 2012

DOI: 10.3892/ijo.2012.1435

Abstract. Human diseases such as Nijmegen breakage syndrome due to mutations in the NBS1 gene result in defects in resection of double strand breaks. NBS1 functions as part of the MRN complex which functions in homologous recombination and non-homologous end joining. NBS is a rare human autosomal recessive disorder caused by hypomorphic mutations. At the cellular level, NBS is characterized by radiosensitivity, chromosomal breakage and defective cell cycle checkpoints. NBS1 null mutations result in early embryonic lethality in mice, but NBS1 hypomorphic mutants are viable. Cells from these mice are defective in S phase and G2/M checkpoints. In humans, NBS1 polymorphisms have been associated with increased risk of breast cancer. MRN expression was reduced in the majority of breast tumors, and low expression of MRN correlated with increased histologic grade and estrogen receptor negativity. While these studies have shown NBS1 to be important in clinical outcomes of patients with breast cancer, mammary tumors are rare in the NBS1 haploinsufficient mouse. To better understand the role of NBS1 in mammary tumorigenesis, we examined the NBS1+/-;MMTV-neu mouse model. Mammary tumor latency was markedly increased in NBS1+/-;neu mice compared to NBS1+/+;neu control animals. This effect was due to increased apoptosis in early NBS1+/-;neu mammary tumors. However, NBS1+/-;neu mammary tumors were highly metastatic and demonstrated clear differences in gene expression profiles compared to control tumors. We concluded that NBS1 haploinsufficiency results in increased mammary tumor latency and metastasis.

Introduction

Double strand break repair is mediated by two major repair pathways, homologous recombination (HR) or non-homologous end joining (NHEJ) (1). In mammalian cells more than 90% of double strand breaks are repaired by NHEJ. Both pathways are defined and their impairment is associated with cell cycle arrest, cell death, genomic instability, and cancer (2). Human diseases such as Nijmegen breakage syndrome due to mutations in the NBS1 gene result in defects in resection of double strand breaks (3). NBS1 functions as part of the MRN complex whose functions are not restricted to HR but are also involved NHEJ (4).

NBS is a rare human autosomal recessive disorder caused by hypomorphic mutations. This disorder is characterized by growth retardation, immunodeficiency, microcephaly, and cancer predisposition. At the cellular level, NBS is characterized by radiosensitivity, chromosomal breakage, and defective cell cycle checkpoints. NBS1 null mutations in mice result in early embryonic lethality (5), but NBS1 hypomorphic mutants are viable (6). Cells from these mice are defective in S phase and G2/M checkpoints. Heterozygous mice with an NBS1 null mutation and homozygous animals with hypomorphic mutations are predisposed to different types of cancer. Conditional NBS1 mutant mice also have been characterized (7). For example, neuronal inactivation of NBS1 results in chromosomal breaks, microcephaly, growth retardation, cerebellar defects, and ataxia.

NBS1 polymorphisms have been associated with increased risk of breast cancer (8-10). MRN expression was reduced in the majority of breast tumors (11), and low expression of MRN correlated with increased histologic grade and estrogen receptor negativity. Response to radiotherapy correlated with high expression of the MRN complex. Patients with high numbers of ionizing radiation induced NBS1 foci had aggressive breast cancer phenotypes (12,13). While these studies have shown NBS1 to be important in clinical outcomes of patients with breast cancer, mammary tumors are rare in the NBS1 haploinsufficient mouse. To better understand the role of NBS1 in mammary tumorigenesis, we characterized these cancers using the NBS1+/-;MMTV-neu mouse.

Materials and methods

Transgenic mouse procedures. Animal procedures were approved by the Institutional Animal Care Committee. NBS1+/- mice (6) were crossed with the mammary tumor prone MMTV-neu transgenic strain in the FVB background (The Jackson Laboratory, Bar Harbor, ME). Tumor development in 30 NBS1+/-;neu mice was compared to that in 30 NBS1+/+;neu

Correspondence to: Dr David L. Crowe, University of Illinois Cancer Center, 801 S. Paulina St., Room 530C, Chicago, IL 60612, USA
E-mail: dlcrowe@uic.edu

Key words: Rad50, Mre11, Nijmegen breakage syndrome 1 gene, MMTV-neu, DNA damage

control mice. Mice were genotyped by PCR analysis of tail DNA samples. The mammary gland chains of female mice were examined visually and by palpation twice weekly. Tumors were measured twice weekly using calipers. Mice were euthanized 4 or 8 weeks after tumor formation followed by complete necropsy. Tumor tissue was processed for histopathologic and gene expression analyses. Statistical analysis was determined by ANOVA.

Mammary gland and tumor histopathology. For whole mount analysis, mammary glands were fixed in 3:1 ethanol:acetic acid, mounted on microscope slides, and stained with carmine-alum followed by clearing in 2:1 benzyl benzoate:benzyl alcohol. Tumor tissue was fixed in formalin for 16 h at room temperature. Tissue was dehydrated in an ethanol series followed by clearing in xylene and embedding in paraffin. Five micrometer sections were cut from the blocks and placed on poly-L-lysine coated slides. Sections were deparaffinized in xylene and stained with hematoxylin and eosin for histopathologic interpretation.

Cellular proliferation and programmed cell death analysis. Mouse mammary tumor tissue was dissociated to single cells by trypsinization, fixed with 2% formaldehyde for 20 min at 4˚C followed by permeabilization with 70% ethanol, then washed with PBS. For proliferation analysis, cells were incubated with anti-PCNA antibody followed by anti-rabbit IgG secondary antibody conjugated to fluorescein. Cells were washed extensively with PBS. For programmed cell death analysis, cells were incubated with terminal deoxynucleotidyl transferase and fluorescein conjugated dUTP at 37˚C for 30 min followed by washing in PBS. The percentage of fluorescein positive cells in each group was determined by flow cytometry.

Reverse transcription-polymerase chain reaction. RNA was extracted from mouse mammary tumors using a commercially available kit (Qiagen, Valencia, CA) and reverse transcribed using SuperScript II reverse transcriptase according to manufacturer's instructions (Invitrogen, Carlsbad, CA). cDNA was amplified using specific primers (5'-3'): Nbs1, TTCCCCCAT ACAAGTATCCAG and AACTTAAGGAGCATCTATGCAG; Malat1, CATCCCGTTCCTTGTTACTC and AGACTACAA ACATTGTGTCGTG; Cdkn2b, GCTAAATGGGAAACC TGGAGAG and ACGTTGAGTCTGTCAGAATCC; Hif1a, CAGCTCCCTTTCTGATAAGC and TCTTCAGTTTCTGT GTCATCG; Egf, TCTGTCAACCCCTGAATAAATG and TTTCACTGGGAAAGACTTCAAG; Lalba, TACCCTGTA GTGACACCACC and TAAAACCCCCATCGAGACC; Jag1, AATGCTGAACCACTTGTAGAC and GGTGAACCT GGATCACTCTG; Areg, TGAATCATTGCCAAGCCAC and TAAAAAGTGACAACTGGGCATC; Csn1s1, CTCCATCC ACCTCATGTCTC and CGCTCAGATGATGCAACTG; Tgfb2, ATGTCTTCAGCCGAGGTCTG and CCCACATC TTCTTTCTCTGCTC; Ccnb2, GTATTACACAGGCTAC ATGGAG and ACATACAGGATCTGAGAAGCG; Dsc2, ATGCTGTGCCTTGCTTTAG and AGCATTTGGTGT TCACAGAC; Csn1s2, TCTTCGTGGTTTCCCCATC and ACTTTAATGTCTTGGCGAGAG in 20 mM Tris-HCl (pH 8.3), 1.5 mM $MgCl_2$, 63 mM KCl, 0.05% Tween 20, 1 mM EGTA, 50 μM of each dNTP, and 2.5 U Taq DNA polymerase (Roche Applied Science, Indianapolis, IN). Amplification with β-actin cDNA using primers 5'-ACAGGAAGTCCCTTGCC ATC-3' and 5'-ACTGGTCTCAAGTCAGTGTACAGG-3' as the internal control was carried out by real-time PCR (iCycler, Bio-Rad) using cycle parameters 94˚C for 25 sec, 55˚C for 1 min, and 72˚C for 1 min.

Global gene expression profiling. Total RNA was extracted from microdissected tumors (n=3 for each group) using a commercially available kit (RNEasy, Qiagen). Integrity of ribosomal RNA bands was confirmed by northern gel electrophoresis. For each hybridization, total RNA (10 μg) was converted to labeled cRNA targets. The biotinylated cRNA targets were then purified, fragmented, and hybridized to GeneChip mouse genome 430 2.0 expression arrays (Affymetrix, Santa Clara, CA) to interrogate the abundance of 39,000 possible transcripts in each sample. Affymetrix GCOS software was used to generate raw gene expression scores and normalized to the relative hybridization signal from each experiment. All gene expression scores were set to a minimum value of 2 times the background determined by GCOS software in order to minimize noise associated with less robust measurements of rare transcripts. Data was analyzed by t-test with $p<0.005$ followed by ratio analysis (minimum 2-fold change).

Results

The histopathology of NBS1+/-;neu mammary glands was consistent with that of NBS1+/+;neu animals, exhibiting normal mammary ductal structure in young mice (Fig. 1A). Mice from both genotypes developed hyperplastic terminal end buds which progressed to poorly differentiated adenocarcinoma (Fig. 1B). Monomorphic sheets of poorly differentiated epithelial cells with duct formation was observed in tumors from both NBS1+/-;neu and NBS1+/+;neu mice (Fig. 1C and D). Lung metastasis was observed in both groups of animals (Fig. 1E). The tumor latency in NBS1+/-;neu mice was dramatically increased (77 weeks vs. 40 weeks for NBS1+/+;neu animals; $p<0.01$; Fig. 2A). However NBS1+/-;neu mammary tumors were highly metastatic (4-fold increase in percentage of mice with metastatic tumors ($p<0.02$; Fig. 2B).

To understand the increased latency of NBS1+/-;neu mammary tumors, we analyzed cellular proliferation and programmed cell death. As shown in Fig. 3A, 4 week NBS1+/-;neu tumors exhibited a 7-fold increase in apoptotic cells as determined by TUNEL analysis. The percentage of apoptotic cells in eight week NBS1+/-;neu tumors was similar to that in NBS1+/+;neu mice. We also analyzed cellular proliferation in early and late stage NBS1+/-;neu and NBS1+/+;neu mammary tumors. We did not detect significant differences in the percentages of PCNA positive cells between these groups (Fig. 3B). We concluded that increased apoptosis in NBS1+/-;neu mammary tumors resulted in increased latency.

To understand the differences in mammary tumor phenotype in NBS1+/-;neu mice, we performed global gene expression profiling. Changes in cancer gene expression are shown in Tables I-III. Primary tumors from NBS1+/-;neu and NBS1+/+;neu were more highly related to each other than to metastatic tumors. Bioinformatic analysis revealed gene expression changes in specific pathways distinguishing NBS1+/-;neu from NBS1+/+;neu primary tumors, including metastasis

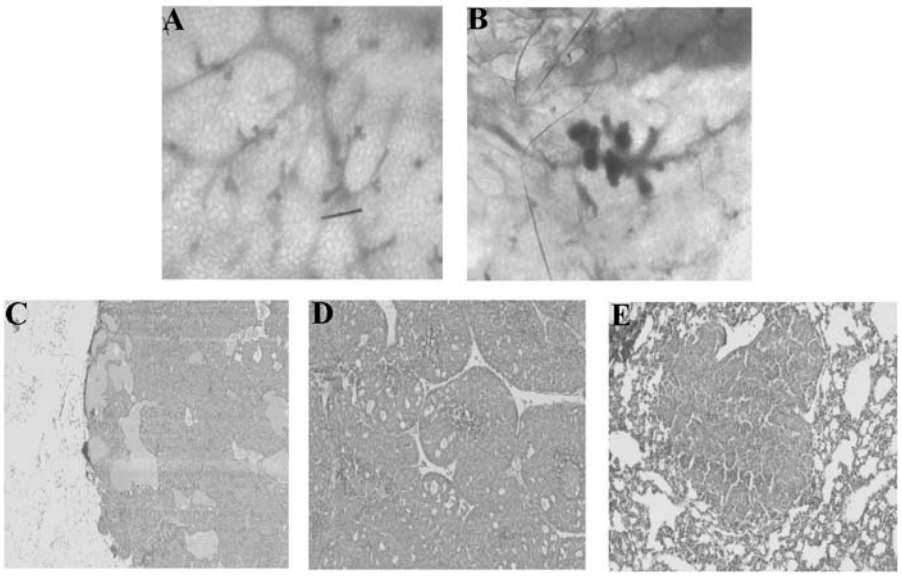

Figure 1. NBS1 haploinsufficiency increases tumor latency in the mammary tumor prone MMTV-neu mouse. (A) Whole mount preparation of mammary fat pad in NBS1+/- mouse. (B) Whole mount preparation of mammary fat pad in NBS1+/-;neu mouse showing hyperplastic terminal end buds. (C) Poorly differentiated adenocarcinoma in the mammary fat pad of NBS1+/-;neu mouse. Section is stained with hematoxylin and eosin; scale bar = 100 μm. (D) Higher magnification of poorly differentiated adenocarcinoma in NBS1+/-;neu mouse. Tumor consists of sheets of poorly differentiated epithelial cells and ducts. Scale bar = 50 μm. (E) Metastatic tumor in lung of NBS1+/-;neu mouse. Magnification is same as in (D).

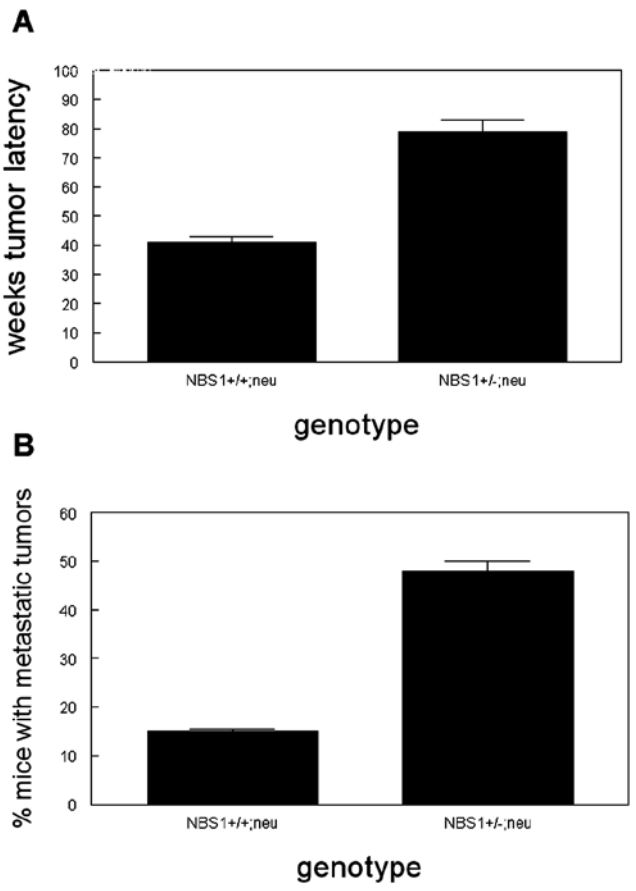

Figure 2. (A) Increased tumor latency in NBS1+/-;neu mice. The number of weeks to tumor formation in NBS1+/+;neu and NBS+/-;neu mice were determined by twice weekly palpation. (B) Increased metastatic mammary cancer in NBS1+/-;neu mice. The percentage of NBS1+/-;neu and NBS1+/+;neu mice with metastatic mammary tumors is shown. Error bars indicate SEM.

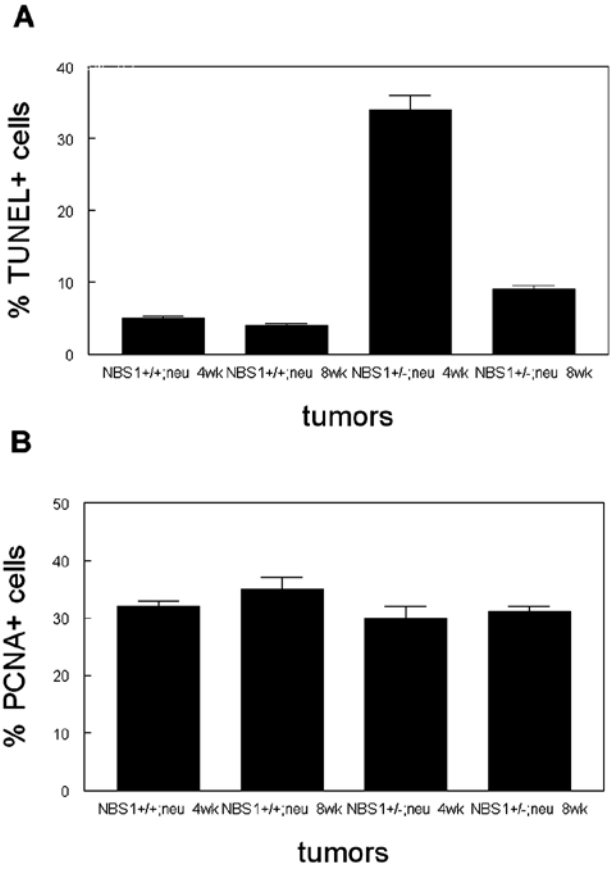

Figure 3. Increased programmed cell death in early NBS1+/-;neu mammary tumors correlates with increased latency. (A) The percentage of apoptotic cells in early and late stage NBS1+/-;neu and NBS1+/+;neu mammary tumors was determined as described in Materials and methods. (B) To assess cellular proliferation, the percentage of PCNA positive cells in early and late stage NBS1+/-;neu and NBS1+/+;neu mammary tumors was determined. Error bars indicate SEM.

Table I. Differentially expressed genes between NBS1+/+;neu and NBS+/-;neu primary mammary tumors (55 genes).

Accession	Gene name	Gene symbol	Fold change
NM_007470	Apolipoprotein D	Apod	796.0
AV325919	ATPase, Na^+/K^+ transporting, α2	Atp1a2	198.9
AF108501	Chloride channel calcium activated 2	Clca2	58.0
NM_030677	Glutathione peroxidase 2	Gpx2	54.1
AF146523	Metastasis lung adenocarcinoma 1	Malat1	43.6
NM_008183	Glutathione S-transferase, mu 2	Gstm1	31.8
NM_134032	Homeo box B2	Hoxb2	18.0
BC011063	Homeo box A5	Hoxa5	17.1
AW105779	Lactate dehydrogenase D	Ldhd	14.6
AV367068	Desert hedgehog	Dhh	13.8
NM_013605	Mucin 1, transmembrane	Muc1	12.2
AF059567	Cyclin-dependent kinase inhibitor 2B	Cdkn2b	11.4
NM_008259	Forkhead box A1	Foxa1	10.5
NM_008608	Matrix metallopeptidase 14	Mmp14	10.3
AI649186	Fibroblast growth factor 1	Fgf1	9.6
U30244	Ephrin B2	Efnb2	9.5
BE686893	Nuclear receptor coactivator 7	Ncoa7	9.0
AB049755	Mannan-binding lectin serine peptidase	Masp1	9.0
BG073383	Homeo box B3	Hoxb3	8.9
NM_008858	Protein kinase C, mu	Prkcm	8.5
BB197591	Protocadherin 7	Pcdh7	8.4
BB224034	Phospholipase C, β4	Plcb4	8.1
BB322941	Nuclear receptor subfamily 4, group A, 2	Nr4a2	7.4
NM_007556	Bone morphogenetic protein 6	Bmp6	7.0
NM_013867	Breast cancer anti-estrogen resistance 3	Bcar3	6.8
BB269715	Hypoxia inducible factor 1, α subunit	Hif1a	6.4
BB795235	Frizzled homolog 5 (*Drosophila*)	Fzd5	6.4
BB795491	DNA methyltransferase 3A	Dnmt3a	6.3
NM_007631	Cyclin D1	Ccnd1	6.3
BC024375	Growth hormone receptor	Ghr	6.2
AA214868	Phosphatase and tensin homolog	Pten	6.2
BB520860	RAR-related orphan receptor α	Rora	6.2
BB376407	Jumonji, AT rich interactive domain 1A	Jarid1a	5.9
AV359819	Jagged 1	Jag1	5.5
NM_008054	Fyn proto-oncogene	Fyn	5.4
AV241297	Serine peptidase inhibitor, Kazal type 5	Spink5	-6.4
NM_010113	Epidermal growth factor	Egf	-8.3
NM_010679	Lactalbumin, α	Lalba	-21.7
NM_009973	Casein α s2-like B	Csn1s2b	-27.2
NM_008644	Mucin 10, salivary mucin	Muc10	-100.4

(Malat1, 43.6-fold; Mmp14, 10.3-fold), cell cycle (Cdkn2b, 11.4-fold), angiogenesis (Hif1a, 6.4-fold), epidermal growth factor signaling (Egf, -8.3-fold), and differentiation (Lalba, -21.7-fold; Csn1s2b, -27.2-fold; Muc10, -100.4-fold). We also compared gene expression in NBS1+/-;neu and NBS1+/+;neu metastatic tumors. These pathways included metastasis, Notch signaling (Dlk1, 462.9-fold; Jag1, 28.6-fold; Jag2, 6.2-fold), epidermal growth factor receptor signaling (Areg, 66.3-fold; Ereg, 23.5-fold; Hbegf, 9.4-fold), fibroblast growth factor signaling (Fgfr2, 68.9-fold; Fgf1, 14.9-fold; Fgfr3, 10.9-fold), peroxisome proliferator activated receptor signaling (Pparg, 21.8-fold; Ppara, 10.1-fold, Ppargc1b, 7.1-fold), forkhead signaling (Foxa2, 42.6-fold; Foxa1, 33.6-fold; Foxp2, 19-fold; Foxq1, 18.1-fold), and differentiation (Wap, -22.1-fold; Csn3, -32.3-fold; Lalba, -212.2-fold; Csn, -310.8-fold; Csn1s1, -365.2-fold). Finally we compared gene expression in primary and metastatic NBS1+/-;neu mammary tumors. These pathways included Notch signaling (Dlk1, 308.8-fold; Jag1, 13.9-fold; Jag2, 6.2-fold), transforming growth factor/

Table II. Differentially expressed genes between NBS1+/+;neu and NBS1+/-;neu metastatic mammary tumors (239 genes).

Accession	Gene name	Gene symbol	Fold change
NM_010052	Δ-like 1 homolog (*Drosophila*)	Dlk1	462.9
NM_007663	Cadherin 16	Cdh16	140.1
NM_008471	Keratin 19	Krt19	98.6
AF146523	Metastasis lung adenocarcinoma 1	Malat1	69.8
NM_010207	Fibroblast growth factor receptor 2	Fgfr2	68.9
NM_009704	Amphiregulin	Areg	66.3
AV304616	Sonic hedgehog	Shh	44.6
NM_010446	Forkhead box A2	Foxa2	42.6
NM_007554	Bone morphogenetic protein 4	Bmp4	34.7
BF585144	Regulator of G-protein signaling 5	Rgs5	34.1
NM_008259	Forkhead box A1	Foxa1	33.6
AV022238	Chemokine (C-X-C motif) ligand 15	Cxcl15	32.7
NM_008398	Integrin α7	Itga7	30.2
AV359819	Jagged 1	Jag1	28.6
NM_007950	Epiregulin	Ereg	23.5
NM_011146	Peroxisome proliferator receptor γ	Pparg	21.8
U30244	Ephrin B2	Efnb2	21.4
NM_133721	Integrin α9	Itga9	20.7
BC002073	Chemokine (C-C motif) ligand 6	Ccl6	19.6
NM_019932	Chemokine (C-X-C motif) ligand 4	Cxcl4	19.4
NM_017399	Fatty acid binding protein 1, liver	Fabp	19.4
AV322952	Forkhead box P2	Foxp2	19.0
AV009267	Forkhead box Q1	Foxq1	18.1
AI649186	Fibroblast growth factor 1	Fgf1	14.9
NM_013867	Breast cancer anti-estrogen resistance 3	Bcar3	13.1
AV239587	Bone morphogenetic protein 2	Bmp2	11.8
NM_008010	Fibroblast growth factor receptor 3	Fgfr3	10.9
NM_008608	Matrix metallopeptidase 14	Mmp14	10.8
BB277517	Histone deacetylase 7A	Hdac7a	10.3
BC016892	Peroxisome proliferator receptor α	Ppara	10.1
BG069466	CREB binding protein	Crebbp	9.8
NM_013565	Integrin α3	Itga3	9.6
BB040443	Snail homolog 2 (*Drosophila*)	Snai2	9.5
L07264	Heparin-binding EGF-like growth factor	Hbegf	9.4
AK004683	Wingless-related MMTV integration 7A	Wnt7a	8.8
BM239177	Mitogen activated protein kinase 14	Mapk14	8.7
BC010202	Kirsten rat sarcoma viral oncogene	Kras	8.6
BB376407	Jumonji, AT rich interactive domain 1A	Jarid1a	8.2
BM119402	Sloan-Kettering viral oncogene homolog	Ski	7.7
NM_133249	Peroxisome receptor coactivator 1β	Ppargc1b	7.1
BC011118	CCAAT/enhancer binding protein α	Cebpa	6.8
NM_020265	Dickkopf homolog 2 (*Xenopus laevis*)	Dkk2	6.8
NM_008416	JunB oncogene	JunB	6.5
AV264681	Jagged 2	Jag2	6.2
BG064099	Braf transforming gene	Braf	5.8
NM_007669	Cyclin-dependent kinase inhibitor 1A	Cdkn1a	-6.1
BF144658	Transforming growth factor, β2	Tgfb2	-6.7
AU043193	Frizzled homolog 3 (*Drosophila*)	Fzd3	-6.9
BC008152	Caspase 1	Casp1	-13.3
NM_009808	Caspase 12	Casp12	-13.8
NM_011709	Whey acidic protein	Wap	-22.1
BC004601	Casein κ	Csn3	-32.3
NM_010679	Lactalbumin, α	Lalba	-212.2
NM_009972	Casein β	Csn	-310.8
NM_007784	Casein α s1	Csn1s1	-365.2

Table III. Differentially expressed genes between NBS1+/-;neu primary and metastatic tumors (222 genes).

Accession	Gene name	Gene symbol	Fold change
AV022238	Chemokine (C-X-C motif) ligand 15	Cxcl15	405.0
NM_010052	Δ-like 1 homolog (*Drosophila*)	Dlk1	308.8
BC002073	Chemokine (C-C motif) ligand 6	Ccl6	113.2
NM_008471	Keratin 19	Krt19	111.5
AV304616	Sonic hedgehog	Shh	104.9
NM_010446	Forkhead box A2	Foxa2	81.7
NM_007554	Bone morphogenetic protein 4	Bmp4	69.4
NM_008010	Fibroblast growth factor receptor 3	Fgfr3	24.8
NM_007950	Epiregulin	Ereg	23.5
NM_008404	Integrin β2	Itgb2	21.9
NM_011126	Palate, lung and nasal carcinoma	Plunc	20.1
AK007410	Growth arrest and DNA-damage 45	Gadd45g	18.3
AV009267	Forkhead box Q1	Foxq1	18.1
BC011118	CCAAT/enhancer binding protein α	Cebpa	15.4
AF416641	Hypoxia inducible factor 3, α subunit	Hif3a	15.0
AA880220	Jagged 1	Jag1	13.9
AV322952	Forkhead box P2	Foxp2	12.8
NM_010207	Fibroblast growth factor receptor 2	Fgfr2	12.3
AV311104	Cancer susceptibility candidate 4	Casc4	11.3
BM231135	Bone morphogenetic protein 1	Bmp1	11.2
NM_013565	Integrin α3	Itga3	10.3
AV032115	Bone morphogenetic protein 5	Bmp5	8.6
AF128196	Chemokine (C-C motif) ligand 9	Ccl9	8.2
NM_008261	Hepatic nuclear factor 4, α	Hnf4a	7.7
NM_011332	Chemokine (C-C motif) ligand 17	Ccl17	7.5
NM_008259	Forkhead box A1	Foxa1	7.3
BB373572	Calcium dependent protein kinase II	Camk2d	7.0
NM_020265	Dickkopf homolog 2 (*Xenopus laevis*)	Dkk2	6.8
BB486740	Hypoxia inducible factor 3, α subunit	Hif3a	6.7
BM293452	Jumonji, AT rich interactive domain 2	Jarid2	6.5
AV264681	Jagged 2	Jag2	6.2
M65143	Lysyl oxidase	Lox	6.0
NM_133654	CD34 antigen	Cd34	6.0
BC005453	V-myc viral related oncogene	Mycn	5.8
BE688115	Fibroblast growth factor 1	Fgf1	5.6
BB787243	Insulin-like growth factor binding protein	Igfbp4	5.6
BC023427	Platelet derived growth factor, B	Pdgfb	5.5
BB015508	Jumonji domain containing 1C	Jmjd1c	5.4
BB040443	Snail homolog 2 (*Drosophila*)	Snai2	5.2
BQ175880	Cyclin D2	Ccnd2	5.0
BB543291	Chemokine (C-C motif) receptor-like 1	Ccrl1	5.0
NM_011121	Polo-like kinase 1 (*Drosophila*)	Plk1	-5.4
BC027242	Vav 3 oncogene	Vav3	-5.8
X75483	Cyclin A2	Ccna2	-5.8
BC003261	Aurora kinase B	Aurkb	-6.8
NM_009525	Wingless-related integration site 5B	Wnt5b	-6.9
BF144658	Transforming growth factor, β2	Tgfb2	-8.4
NM_019645	Plakophilin 1	Pkp1	-8.4
AK013312	Cyclin B2	Ccnb2	-8.4
AV367068	Desert hedgehog	Dhh	-8.8
AU043193	Frizzled homolog 3 (*Drosophila*)	Fzd3	-10.5
NM_013505	Desmocollin 2	Dsc2	-11.9
U03425	Epidermal growth factor receptor	Egfr	-18.5
BC014690	Transforming growth factor, β3	Tgfb3	-29.2
NM_007785	Casein α s2-like A	Csn1s2a	-127.4
NM_009972	Casein β	Csn	-160.8
NM_007786	Casein κ	Csn3	-958.5

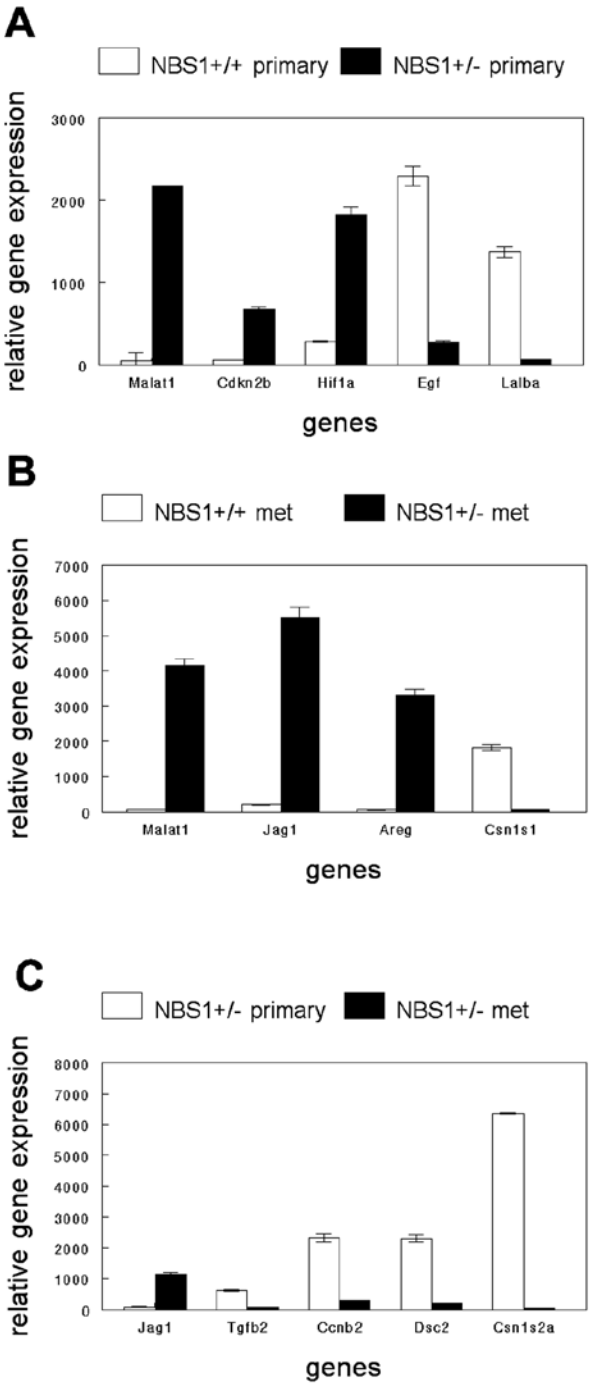

Figure 4. NBS1+/-;neu mammary tumors exhibit specific gene expression signatures. (A) Relative mRNA expression of genes in NBS1+/+;neu and NBS1+/-;neu primary mammary tumors was performed by qRT-PCR. (B) Relative mRNA expression of genes in NBS1+/+;neu and NBS1+/-;neu metastatic mammary tumors was performed by qRT-PCR. (C) Relative mRNA expression of genes in NBS1+/-;neu primary and metastatic mammary tumors was performed by qRT-PCR. Error bars indicate SEM.

bone morphogenetic protein signaling (Bmp4, 69.4-fold; Bmp1, 11.2-fold; Bmp5, 8.6-fold; Tgfb2, -8.4-fold), cell cycle (Ccnd2, 5-fold; Ccna2, -5.8-fold; Ccnb2, -8.4-fold), cell adhesion (Pkp1, -8.4-fold; Dsc2, -11.9-fold), forkhead signaling (Foxa2, 81.7-fold; Foxq1, 18.1-fold; Foxp2, 12.8-fold), epidermal growth factor signaling (Ereg, 23.5-fold; Egfr, -18.5-fold), and differentiation (Csn1s2a, -127.4-fold; Csn -160.8-fold; Csn3, -958.5-fold). Expression of representative genes involved in these pathways was validated by qRT-PCR in Fig. 4. These results demonstrated specific patterns of gene expression that correlated with primary and metastatic tumor phenotype.

Discussion

Mutations in the NBS1 gene have been associated with increased risk of breast cancer (14-16). Persistent radiation induced NBS1 foci has been associated with chromosomal instability and increased breast cancer risk (13). In mice, NBS1 null mutation is embryonic lethal but heterozygosity renders mice susceptible to tumor formation (5). However, mammary tumors are uncommon in mouse strains with reduced NBS1 function (6). To examine the role of NBS1 in mammary tumor formation, we examined NBS1 haploinsufficiency in the mammary tumor prone MMTV-neu strain. Reduced expression of NBS1 resulted in increased apoptosis in NBS1 heterozygous mice. This increased cell death correlated with markedly increased tumor latency in NBS1 heterozygous mice. These effects were likely due to decreased DNA repair following oncogene induced cellular proliferation. Defects in cellular proliferation were noted in the cells of NBS1 deficient mice in previous studies (6). Increased latency correlated with decreased growth factor expression and increased cyclin dependent kinase inhibitor expression. Loss of p53 has been shown to greatly increase tumorigenesis in NBS1 mutant mice, suggesting that p53 mediated DNA damage response may be responsible for apoptosis and increased tumor latency (15). A previous study demonstrated nuclear export of NBS1 following ionizing radiation as a mechanism of downregulating the DNA damage response (16). Previous studies have demonstrated increased chromosomal aberrations in NBS1+/- tumors (5). Loss of NBS1 has been shown to induce supernumerary centrosomes similar to those observed in BRCA1 deficient cells, leading to increased chromosomal instability (17). These studies demonstrate that impaired NBS1 function can result in cellular proliferation defects leading to increased tumor latency. It is interesting to speculate that tumorigenic clones that escape defective cell death pathways may be more aggressive and metastatic due to chromosomal aberrations induced by diminished NBS1 function. In support this hypothesis, increased numbers of differentially expressed genes and degregulated signaling pathways in NBS1+/-;neu tumors correlated with increased metastatic disease.

Acknowledgements

We thank Dr Yang Xu (University of California San Diego) for NBS1 mutant mice. This study was supported by Susan G. Komen for the Cure award BCTR0504295 and Department of Defense Breast Cancer Research Program award W81XWH-10-1-0081 to D.L.C.

References

1. Barlev NA, Liu L, Chehab NH, Mansfield K, Harris KG, Halazonetis TD and Berger SL: Acetylation of p53 activates transcription through recruitment of coactivators/histone acetyltransferases. Mol Cell 8: 1243-1254, 2001.

2. Bartkova J, Tommiska J, Oplustilova L, Aaltonen K, Tamminen A, Heikkinen T, Mistrik M, Aittomaki K, Blomqvist C, Heikkila P, Lukas J, Nevanlinna H and Bartek J: Aberrations of the MRE11-RAD50-NBS1 DNA damage sensor complex in human breast cancer: MRE11 as a candidate familial cancer predisposing gene. Mol Oncol 2: 296-316, 2008.
3. Bogdanova N, Feschchenko S, Schurmann P, Waltes R, Wieland B, Hillemanns P, Rogov YI, Dammann O, Bremer M, Karstens JH, Sohn C, Varon R and Dork T: Nijmegen breakage syndrome mutations and risk of breast cancer. Int J Cancer 122: 802-806, 2008.
4. Cai BH, Chen JY, Lu MH, Chang LT, Lin HC, Chang YM and Chao CF: Functional four base A/T gap core sequence CATTAG of p53 response elements specifically bound tetrameric p53 differently than two base A/T gap core sequence CATG bound both dimeric and tetrameric p53. Nuc Acids Res 37: 1984-1990, 2009.
5. Chiang YC, Teng SC, Su YN, Hsieh FJ and Wu KJ: c-myc directly regulates the transcription of the NBS1 gene involved in DNA double strand break repair. J Biol Chem 278: 19286-19291, 2003.
6. Crowe DL and Lee MK: New role for nuclear hormone receptors and coactivators in regulation of BRCA1 mediated DNA repair in breast cancer cell lines. Breast Cancer Res 8: 1-12, 2006.
7. Dumon-Jones V, Frappart PO, Tong WM, Sajithlal G, Hulla W, Schmid G, Herceg Z, Digweed M and Wang ZQ: Nbn heterozygosity renders mice susceptible to tumor formation and ionizing radiation induced tumorigenesis. Cancer Res 63: 7263-7269, 2003.
8. Eggleston P and Zhao Y: A sensitive and rapid assay for homologous recombination in mosquito cells: impact of vector topology and implications for gene targeting. BMC Genet 2: 21-29, 2001.
9. Frappart PO, Tong WM, Demuth I, Radovanovic I, Herceg Z, Aguzzi A, Digweed M and Wang ZQ: An essential function for NBS1 in the prevention of ataxia and cerebellar defects. Nature Med 11: 538-544, 2005.
10. Goodman RH and Smolik S: CBP/p300 in cell growth, transformation, and development. Genes Dev 14: 1553-1577, 2000.
11. Hakem R: DNA damage repair; the good, the bad, and the ugly. EMBO J 27: 589-605, 2008.
12. Hsu HM, Wang HC, Chen ST, Hsu GC, Shen CY and Yu JC: Breast cancer risk is associated with the genes encoding the DNA double strand break repair Mre11/Rad50/Nbs1 complex. Cancer Epidemiol Biomarkers Prev 16: 2024-2032, 2007.
13. Kang J, Bronson RT and Xu Y: Targeted disruption of NBS1 reveals its roles in mouse development and DNA repair. EMBO J 21: 1447-1455, 2002.
14. Nowak J, Mosor M, Ziolkowska I, Wierzbicka M, Pernak-Schwarz M, Przyborska M, *et al*: Heterozygous carriers of the I171V mutation of the NBS1 gene have a significantly increased risk of solid malignant tumors. Eur J Cancer 44: 627-630, 2008.
15. Kang J, Ferguson D, Song H, Bassing C, Eckersdorff M, Alt FW and Xu Y: Functional interaction of H2AX, NBS1, and p53 in ATM dependent DNA damage responses and tumor suppression. Mol Cell Biol 25: 661-670, 2005.
16. Vissinga CS, Yeo TC, Warren S, Brawley JV, Phillips J, Cerosaletti K and Concannon P: Nuclear export of NBN is required for normal cellular responses to radiation. Mol Cell Biol 29: 1000-1006, 2009.
17. Shimada M, Sagae R, Kobayashi J, Habu T and Komatsu K: Inactivation of the Nijmegen breakage syndrome gene leads to excess centrosome duplication via the ATR/BRCA1 pathway. Cancer Res 69: 1768-1775, 2009.